From Recommender Systems to 5D Seismic Data Reconstruction

Mauricio D Sacchi
Department of Physics
University of Alberta

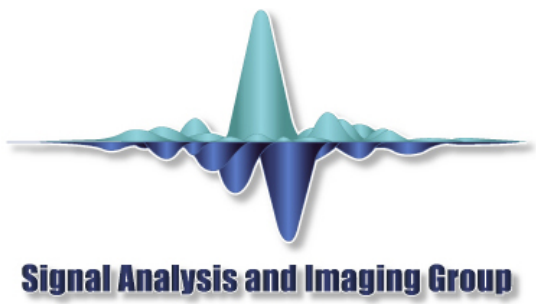

People who have contributed to the project

- Vicente Oropeza - UofA and now Shell
- Jianjun Gao - UofA and now CUG-Beijing
- Aaron Stanton - UofA
- Nadia Kreimer - UofA and now Shell
- Kevin Cheng - UofA
- Ke Chen -UofA

Introduction

- Brief introduction to Matrix and Tensor Completion
- Can we use Tensor Completion techniques to denoise and reconstruct multidimensional (5D) seismic data?
- Examples

Recent progress in "Data Processing"

Compressive Sensing

Matrix/Tensor Completion

Compressive Sensing (Sub-Nyquist sampling)

Given a small number of observation of y, the goal is to recover x by solving the following underdetermined problem:

$$Sx = y$$

If x can be represented as a linear combination of coefficients c (synthetis operator)

$$SAc = y$$

x can be recovered from y for certain class of operators SA if c is sparse.
Solution:

minimize $|c|_1$ subject to $|SAx - y| < \epsilon$

Candes, Romberg, Tao (2006). "Stable signal recovery from incomplete and inaccurate measurements". Communications

Matrix Completion and the Netflix Prize

Movie →

User ↓

	Taxi Driver	Sense and Sensibility	Battleship Potemkin	Raging Bull	Titanic	Alexander Nevsky
John	5	1	5	4	1	3
Mary	1	4	?	1	4	?
Pepe	4	2	2	3	4	?
Adrian	3	1	?	3	3	?
Tony	?	?	?	?	4	?
Kevin	3	3	?	3	2	?
Jianjung	2	1	?	2	4	?
Natasha	?	?	3	?	5	3

Figure: Netflix provided a training data set of 100,480,507 ratings that 480,189 users gave to 17,770 movies (only 1.17% of the elements of the data table/matrix are known)

Matrix Completion and the Netflix Prize

$M^{obs}_{i,j}$: Observed entries of the table
$M_{i,j}$: Desired table

$$M^{obs}_{i,j} = T_{i,j} M_{i,j}$$

$T_{i,j} = 1$ if user i rated movie j
$T_{i,j} = 0$ if user i did not rate movie j

Estimating $M_{i,j}$ from $M^{obs}_{i,j}$ is called a Matrix Completion Problem

Matrix Completion and the Netflix Prize

- From `http://www.netflixprize.com/`: " The Netflix Prize sought to substantially improve the accuracy of predictions about how much someone is going to enjoy a movie based on their movie preferences"
- On September 21, 2009 Netflix awarded the $1M Grand Prize to team BellKors Pragmatic Chaos
- See **Matrix Completion Problem**
- See also Collaborative Filtering Techniques

Netflix Prize

The *Napoleon Dynamite* problem: The movie has been rated more than two million times in the Netflix database with ratings that are disproportionately one or five stars.

Seismic data in source-receiver coordinates

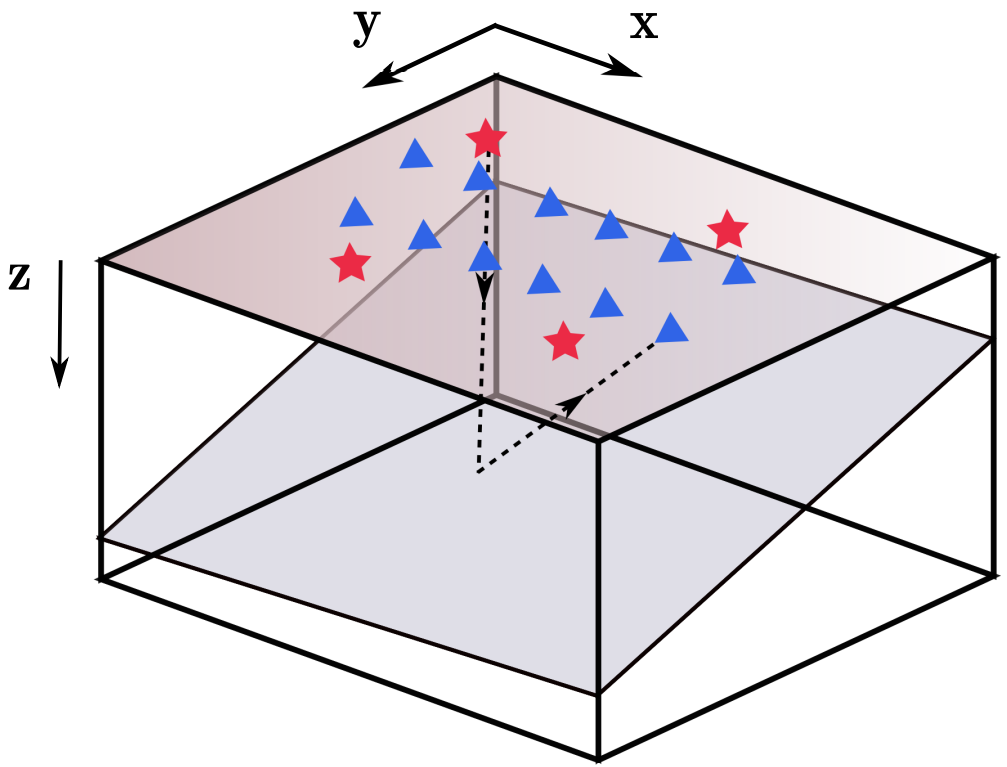

$$d(s_x, s_y, r_x, r_y, t) \rightarrow D(s_x, s_y, r_x, r_y, \omega)$$

Seismic data in midpoint-offset coordinates

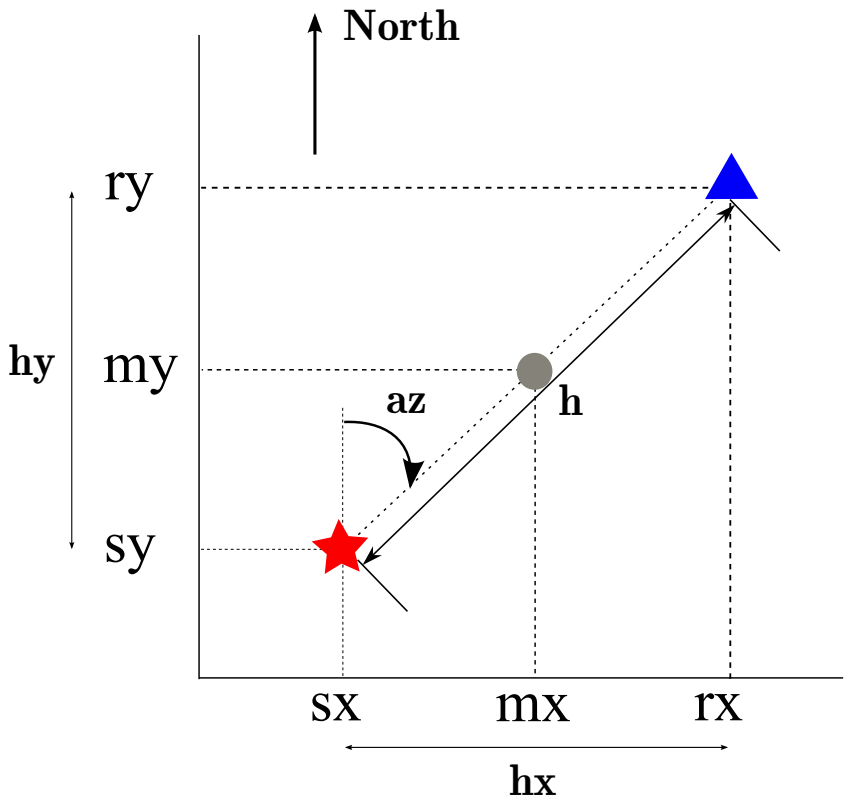

$$d(s_x, s_y, r_x, r_y, t) \rightarrow D(s_x, s_y, r_x, r_y, \omega) \rightarrow D(m_x, m_y, h_x, h_y, \omega)$$

$$D(m_x, m_y, h_x, h_y, \omega) \rightarrow \text{Binning} \rightarrow \mathcal{D}_{i,j,k,l}(\omega)$$

We will simplify notation by calling the seismic data $\mathcal{D}$, a 4-th order multilinear array or tensor. Reconstruction and denoising is carried out for all frequencies $\omega \in [\omega_{min}, \omega_{max}]$.

Source-receiver acquisition WCSB

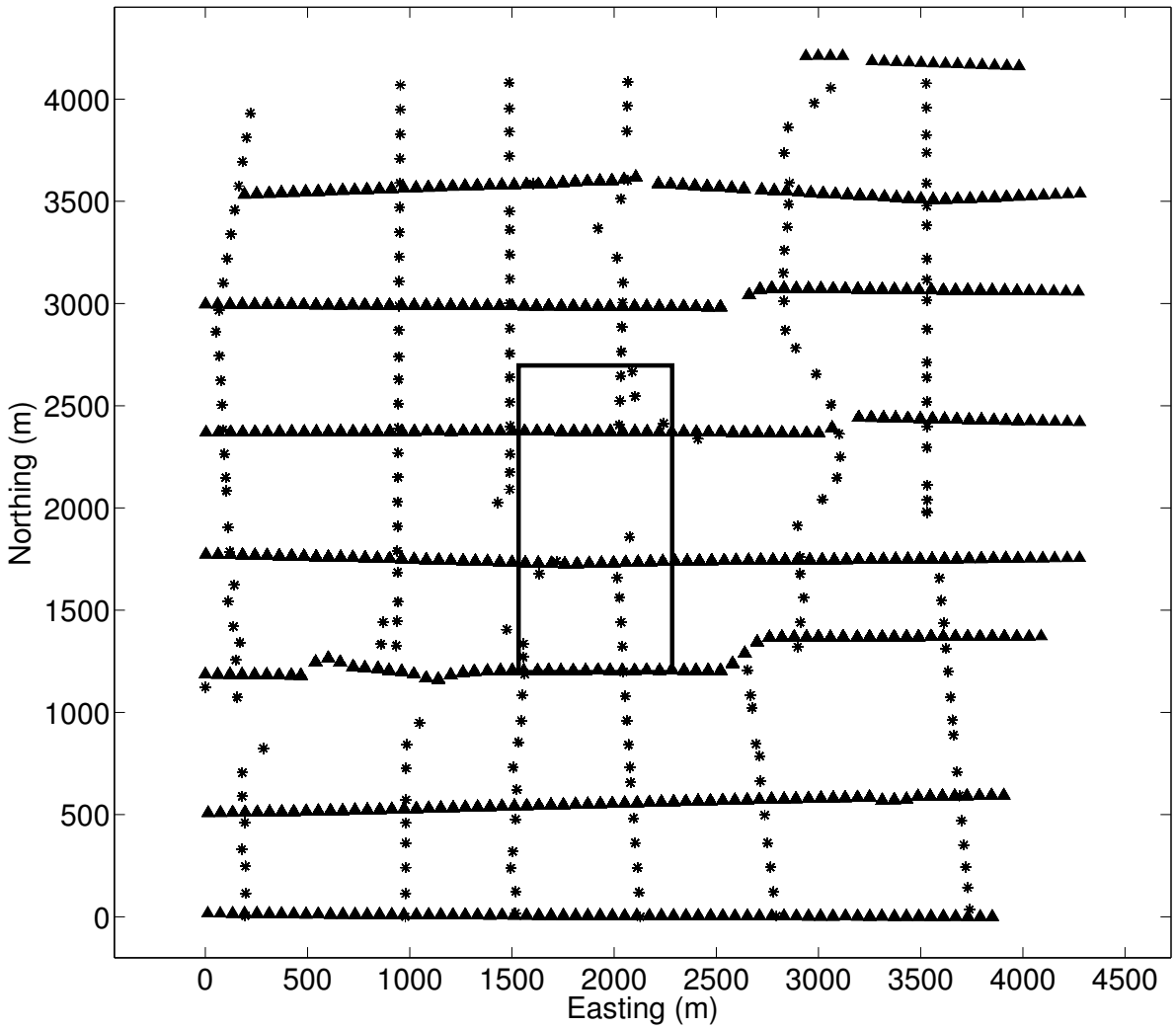

Source-receiver acquisition WCSB

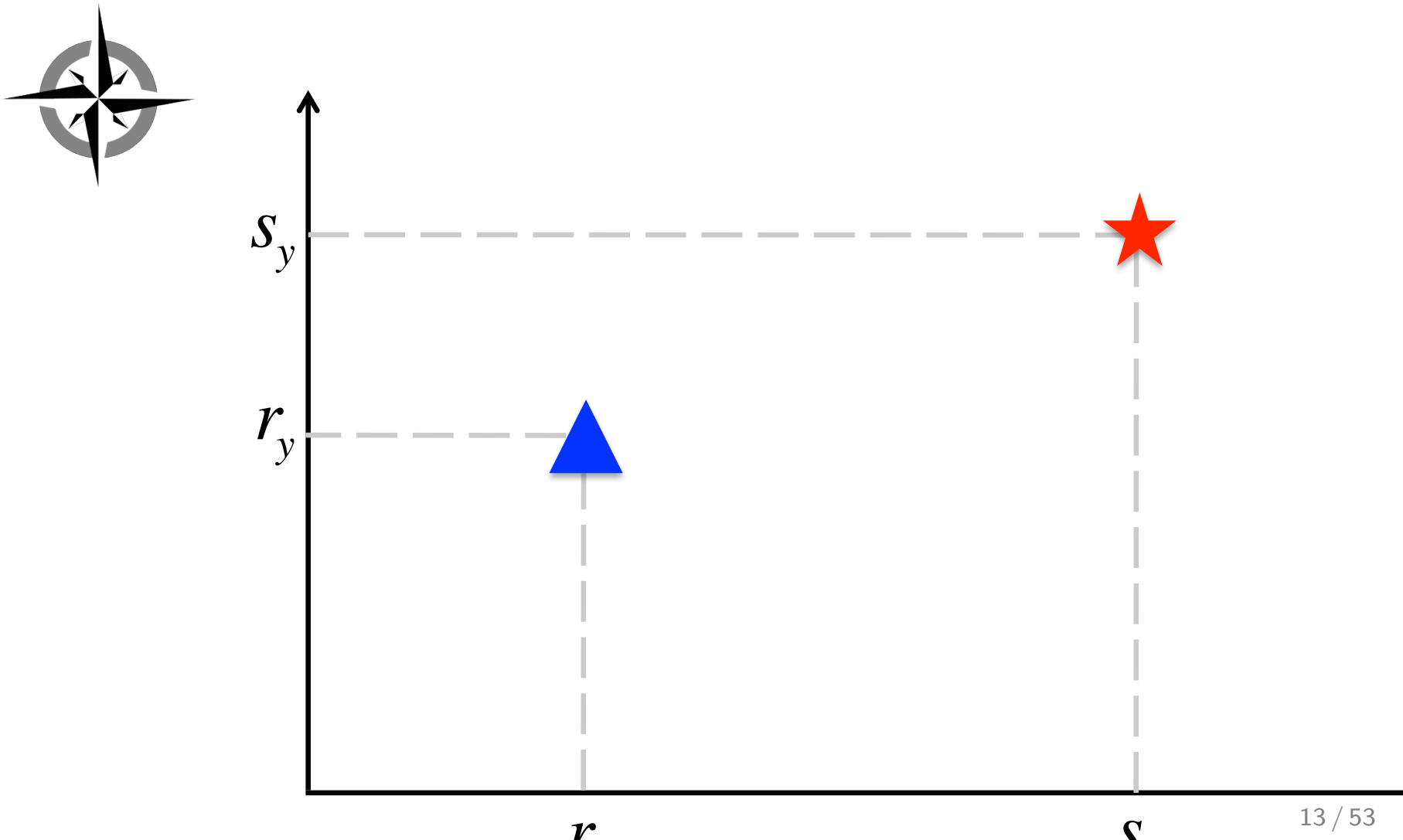

Source-receiver acquisition WCSB: Fold Map

Visualization of 4th seismic order tensor

$$\mathcal{D}^{obs}_{i,j,k,l} = \mathcal{T}_{i,j,kl}\,\mathcal{D}_{i,j,k,l}$$

$$F_{i,j} = \sum_{k,l} \mathcal{T}_{i,j,k,l}$$

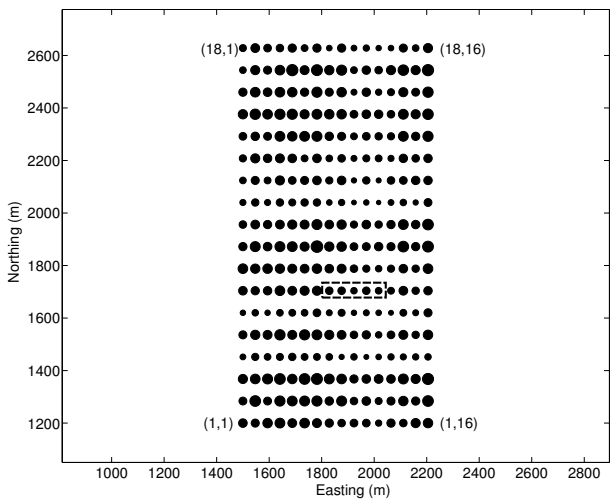

Figure: Fold $F_{i,j}$

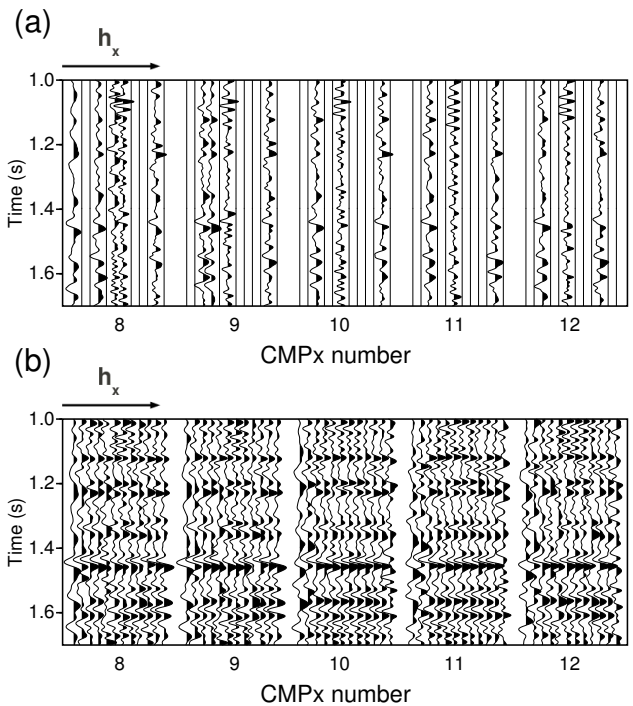

Tensor Completion Problem: Recover $\mathcal{D}$ from $\mathcal{D}^{obs}$. Like Netflix but with Seismic

Seismic data reconstruction

- The majority of industrial codes for data reconstruction are based on Fourier Synthesis: They all invoke sparsity in the wavenumber domain and utilize solvers like IRLS (MWNI) and Matching Pursuit (ALFT).
- As per today, there exits 10^{10} industrial methods for Fourier reconstruction (could use other basis functions), all are extremely similar.
- Completion methods based on rank-reduction
  - Hankel Methods
  - Tensor Methods

Seismic data reconstruction

- Hankel Methods
  - Trickett, S., L. Burroughs, A. Milton, L. Walton, and R. Dack, 2010, Rank-reduction-based trace interpolation: SEG, Expanded Abstracts, 29, no. 1, 3829-3833.
  - Oropeza, V., and M. Sacchi, 2011, Simultaneous seismic data denoising and reconstruction via multichannel singular spectrum analysis: Geophysics, 76, no. 3, V25-V32.
  - Gao, J., M. Sacchi, and X. Chen, 2013, A fast reduced-rank interpolation method for prestack seismic volumes that depend on four spatial dimensions: Geophysics, 78, no. 1, V21-V30.
- Tensor Methods
  - Kreimer, N., and M. D. Sacchi, 2012, A tensor higher-order singular value decomposition for prestack seismic data noise reduction and interpolation: Geophysics, 77, no. 3, V113-V122.

High Order SVD (Kreimer and Sacchi GEO-2012)

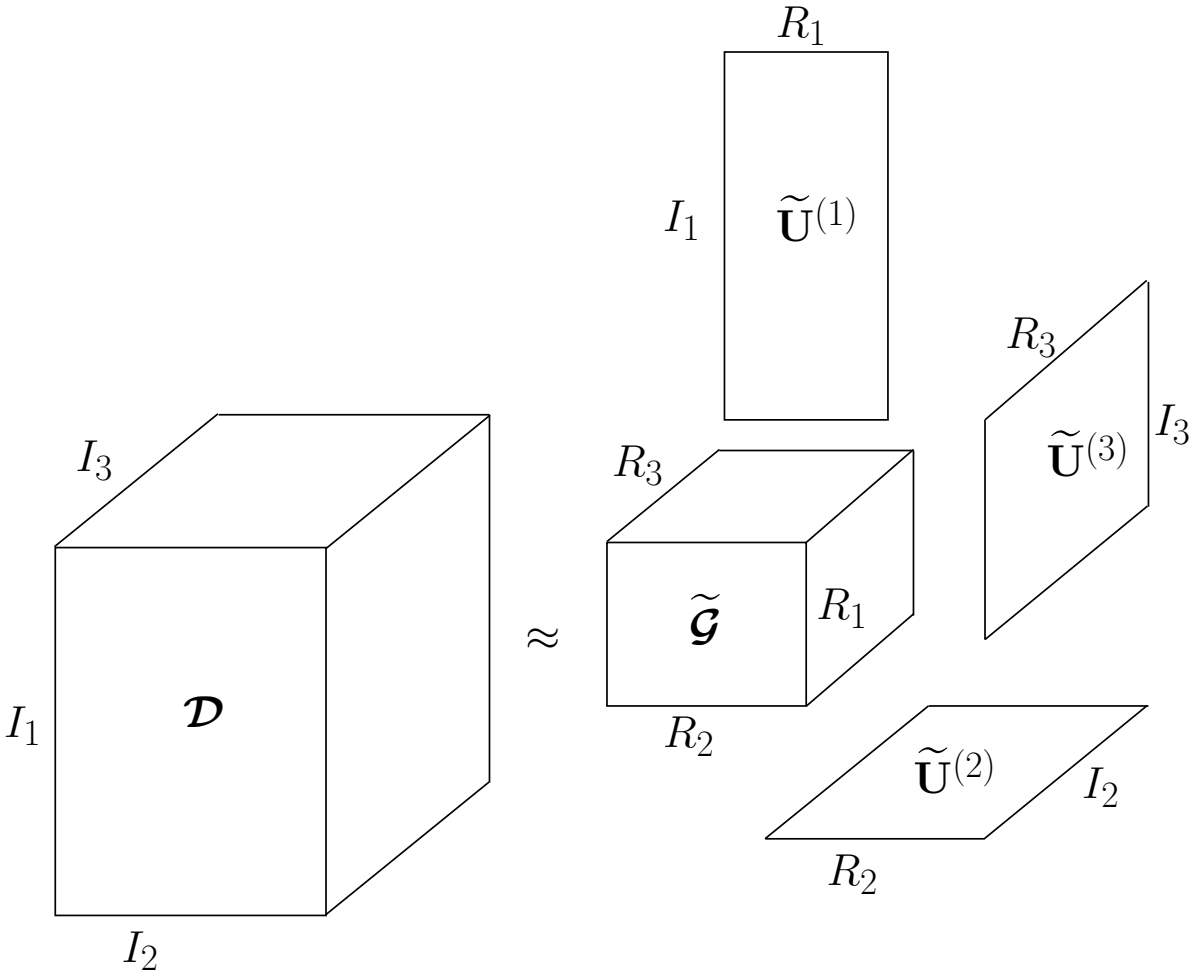

Figure: *

HOSVD

High Order SVD (Kreimer and Sacchi GEO-2012)

Iterative rank reduction via a simple algorithm (no cost function associated to the problem)

$$D^k = D^{obs} + (1 - S)\mathcal{R}D^{k-1}$$

S: Sampling Operator
$\mathcal{R}$: Rank-Reduction Operator (HO-SVD)

Tons of paper in Chemometrics, see for instance, G. Tomasi and R. Bro. PARAFAC and missing values. Chemom.Intell.Lab.Syst. 75:163-180, 2005.

Unfolding

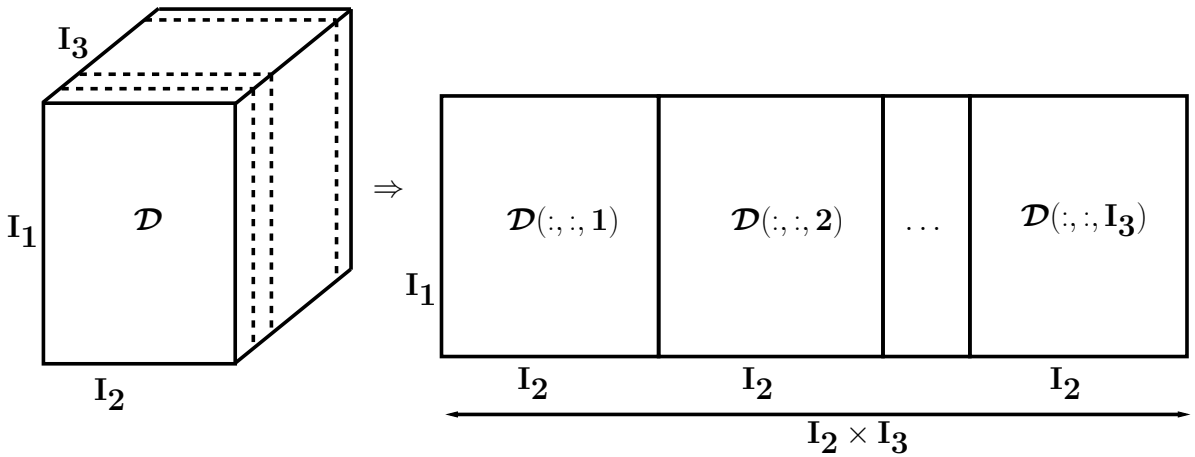

Figure: *

A 3rd order tensor can be unfolded in 3 matrices. This figure shows unfolding in mode 1

Tensor completion via nuclear norm minimization

$$\text{minimize} \quad \sum_{i=1}^{4} \text{rank}(\mathbf{D}^{(i)}) \quad \text{subject to} \quad \mathcal{T}\boldsymbol{\mathcal{D}} = \boldsymbol{d}^{obs}, \qquad (1)$$

or, the more realistic formulation

$$\text{minimize} \quad \sum_{i=1}^{4} \text{rank}(\mathbf{D}^{(i)}) \quad \text{subject to} \quad ||\mathcal{T}\boldsymbol{\mathcal{D}} - d^{obs}||_2^2 < \epsilon \qquad (2)$$

$\mathbf{D}^{(i)}$ is the unfolding of the tensor $\mathcal{D}$ in the mode i
This is an NP-hard problem.

Tensor completion via nuclear norm minimization

Change rank constraint by nuclear norm (sum of the singular values)

$$\text{minimize} \quad J = \sum_{i=1}^{4} \|\mathbf{D}^{(i)}\|_* + \frac{\lambda}{2} \|\mathcal{T}\boldsymbol{\mathcal{D}} - \boldsymbol{d}^{obs}\|_F^2,$$

CS analogy: Turn non-convex NP-hard problem into a tractable convex optimization problem

$l_0 \rightarrow l_1$
rank $\rightarrow$ Nuclear norm $= \|\mathbf{D}^{(i)}\|_* = \sum_k \sigma_k^i$

Fazel, M., H. Hindi, and S. Boyd, 2001, A rank minimization heuristic with application to minimum order system approximation: Proceedings of the 2001 American Control Conference, 6, 4734 4739.

Alternating direction method of multipliers (ADMM)

$$\min_{\mathbf{x}\in\mathbb{C}^q,\,\mathbf{y}\in\mathbb{C}^p} \quad f(\mathbf{x}) + g(\mathbf{y}) \;\text{ such that }\; \mathbf{x}\in C_x,\, \mathbf{y}\in C_y,\; \mathbf{G}\mathbf{x}=\mathbf{y}, \tag{3}$$

where f, g are convex functions, $\mathbf{G}$ is a matrix and C_x, C_y are nonempty polyhedral sets, defined as convex sets formed by a finite collection of linear inequalities. The objective function using the traditional method of multipliers is

$$J_m(\mathbf{x},\mathbf{y},\mathbf{w}) = f(\mathbf{x}) + g(\mathbf{y}) - \mathbf{w}^{\mathsf{T}}(\mathbf{G}\mathbf{x}-\mathbf{y}), \tag{4}$$

where $\mathbf{w}$ is a vector of Lagrange multipliers.

Alternating direction method of multipliers (ADMM)

The augmented objective function (called "augmented Lagrangian")

$$J(\mathbf{x}, \mathbf{y}, \mathbf{w}) = f(\mathbf{x}) + g(\mathbf{y}) - \mathbf{w}^{\mathsf{T}}(\mathbf{G}\mathbf{x} - \mathbf{y}) + \frac{\beta}{2}\|\mathbf{G}\mathbf{x} - \mathbf{y}\|_2^2, \quad (5)$$

Alternating direction method of multipliers (ADMM)

The minimization of J is carried out via the following alternate minimization algorithm

$$\mathbf{x}^{j+1} = \underset{\mathbf{x} \in C_x}{\arg\min}\ J(\mathbf{x}, \mathbf{y}^j, \mathbf{w}^j) \tag{6}$$

$$\mathbf{y}^{j+1} = \underset{\mathbf{y} \in C_y}{\arg\min}\ J(\mathbf{x}^{j+1}, \mathbf{y}, \mathbf{w}^j) \tag{7}$$

$$\mathbf{w}^{j+1} = \mathbf{w}^j - \beta\left(\mathbf{G}\mathbf{x}^{j+1} - \mathbf{y}^{j+1}\right) \tag{8}$$

Hestenes, M. R., 1969, Multiplier and gradient methods: Journal of Optimization Theory and Applications, 4, no. 5, 303-320.

ADMM

$$f(\boldsymbol{\mathcal{D}}) = \frac{\lambda}{2} \|\mathcal{T}\boldsymbol{\mathcal{D}} - \boldsymbol{d}^{obs}\|_F^2 \tag{9}$$

$$g(\boldsymbol{\mathcal{Y}}_i) = \sum_{i=1}^{4} \|\mathbf{Y}_i^{(i)}\|_*. \tag{10}$$

$$\boldsymbol{\mathcal{Y}}_1 = \boldsymbol{\mathcal{D}}, \quad \boldsymbol{\mathcal{Y}}_2 = \boldsymbol{\mathcal{D}}, \quad \boldsymbol{\mathcal{Y}}_3 = \boldsymbol{\mathcal{D}}, \quad \boldsymbol{\mathcal{Y}}_4 = \boldsymbol{\mathcal{D}}. \tag{11}$$

ADMM

We use ADMM to minimize

$$J(\boldsymbol{\mathcal{D}}, \boldsymbol{\mathcal{Y}}_i, \boldsymbol{\mathcal{W}}_i) \;=\; \frac{\lambda}{2}\|\mathcal{T}\boldsymbol{\mathcal{D}} - \boldsymbol{d}^{obs}\|_F^2 \;+\; \sum_{i=1}^{4}\left(\|\mathbf{Y}_i^{(i)}\|_* - <\boldsymbol{\mathcal{W}}_i, \boldsymbol{\mathcal{D}} - \boldsymbol{\mathcal{Y}}_i> + \frac{\beta}{2}\|\boldsymbol{\mathcal{D}} - \boldsymbol{\mathcal{Y}}_i\|_F^2\right). \tag{12}$$

ADMM: Minimization with respect to $\mathcal{Y}_i$

The minimum of J with respect to $\mathcal{Y}_i$ can be computed by using the following theorem. Given a matrix $\mathbf{A}$ and a scalar $\tau \geq 0$, let $\mathbf{B}$ be an approximation to $\mathbf{A}$ such that $\mathbf{B}$ has minimum nuclear norm. In other words,

$$\mathbf{B} = \underset{B}{\operatorname{argmin}} \left\{ \|\mathbf{B}\|_* + \frac{1}{2\tau}\|\mathbf{B} - \mathbf{A}\|_F^2 \right\} . \tag{13}$$

The solution to this problem is given by

$$\mathbf{B} = \text{shrink}(\mathbf{A}, \tau) = \mathbf{U}\tilde{\Sigma}\mathbf{V}^{\mathsf{H}} , \tag{14}$$

where

$$\tilde{\Sigma} = \text{diag}[\max(\sigma_1 - \tau, 0) \ldots \max(\sigma_r - \tau, 0)]. \tag{15}$$

with $\mathbf{A} = \mathbf{U}\Sigma\mathbf{V}^{\mathsf{H}}$.

Cai, J.-F., E. J. Candes, and Z. Shen, 2010, A singular value thresholding algorithm for matrix completion: SIAM Journal on Optimization, 20, no. 4, 1956-1982.

ADMM: Minimization with respect to $\mathcal{Y}_i$

The minimum of the objective function given by Equation 12 with respect to $\mathcal{Y}_i$ is denoted $\widetilde{\mathcal{Y}}_i$ and it is given by

$$\widetilde{\mathcal{Y}}_i = \underset{\mathbf{Y}_i^{(i)}}{\arg\min} \left\{ \|\mathbf{Y}_i^{(i)}\|_* - < \mathbf{W}_i^{(i)}, \mathbf{D}^{(i)} - \mathbf{Y}_i^{(i)} > + \frac{\beta}{2} \|\mathbf{D}^{(i)} - \mathbf{Y}_i^{(i)}\|_F^2 \right\}. \tag{16}$$

By completing the square, the last expression can be rewritten as follows

$$\begin{aligned} \widetilde{\mathcal{Y}}_i = \underset{\mathbf{Y}_i^{(i)}}{\arg\min} \Bigg\{ & \|\mathbf{Y}_i^{(i)}\|_* - \frac{1}{2} \|\mathbf{W}_i^{(i)}\|_F^2 + \frac{1}{2} \|\mathbf{W}_i^{(i)}\|_F^2 - < \mathbf{W}_i^{(i)}, \mathbf{D}^{(i)} - \mathbf{Y}_i^{(i)} > \\ & + \frac{\beta}{2} \|\mathbf{D}^{(i)} - \mathbf{Y}_i^{(i)}\|_F^2 \Bigg\} \\ = \underset{\mathbf{Y}_i^{(i)}}{\arg\min} & \left\{ \frac{1}{\beta} \|\mathbf{Y}_i^{(i)}\|_* + \frac{1}{2} \left\| \mathbf{Y}_i^{(i)} - \left(\mathbf{D}^{(i)} - \frac{1}{\beta} \mathbf{W}_i^{(i)} \right) \right\|_F^2 - \frac{1}{\beta} \|\mathbf{W}_i^{(i)}\|_F^2 \right\}. \end{aligned} \tag{17}$$

The last term in Equation 17 is a constant and is unaffected by the derivative with respect to $\mathbf{Y}_i^{(i)}$. Using the property in expression 14, the minimum for $\mathcal{Y}_i$ is

$$\widetilde{\mathcal{Y}}_i = \text{fold} \left(\text{shrink} \left(\mathbf{D}^{(i)} - \frac{1}{\beta} \mathbf{W}_i^{(i)}, \frac{1}{\beta} \right) \right), \tag{18}$$

ADMM: Minimization with respect to $\mathcal{D}$

To find $\mathcal{D}$, we consider the other two variables $\mathcal{Y}_i, \mathcal{W}_i$ fixed. The gradient of Equation 12 is

$$\frac{\partial J(\mathcal{D})}{\partial \mathcal{D}} = \lambda \mathcal{T}'(\mathcal{T}\mathcal{D} - \boldsymbol{d}^{obs}) - \sum_{i=1}^{4} \mathcal{W}_i + 4\beta\,\mathcal{D} - \sum_{i=1}^{4} \beta\,\mathcal{Y}_i \tag{19}$$

where $\mathcal{T}'$ denotes an operator that maps from $\mathbb{C}^m \rightarrow \mathbb{C}^{I_1 \times I_2 \times I_3 \times I_4}$. This operator obeys $\mathcal{T}'\boldsymbol{d}^{obs} = \mathcal{D}^{obs}$ and satisfies the following property

$$\mathcal{T}'\mathcal{T}(\mathcal{D})\big|_{ijkl} = \begin{cases} D_{ijkl} & \text{if } ijkl \text{ contains an observation} \\ 0 & \text{if } ijkl \text{ is empty} \end{cases} \tag{20}$$

Setting Equation 19 equal to zero, we obtain

$$\widetilde{\mathcal{D}} = (\lambda \mathcal{T}'\mathcal{T} + 4\beta\,\mathcal{I})^{-1} \left[\sum_{i=1}^{4} \mathcal{W}_i + \sum_{i=1}^{4} \beta\,\mathcal{Y}_i + \lambda\,\mathcal{T}'\boldsymbol{d}^{obs} \right].$$

ADMM: Minimization with respect to $\mathcal{D}$

If $\mathcal{A}$ represents the argument in brackets in Equation 21, the inverse of $(\lambda \mathcal{T}'\mathcal{T} + 4\beta\mathcal{I})$ depends on which element of tensor $\mathcal{A}$ it is applied to

$$[(\lambda \mathcal{T}'\mathcal{T} + 4\beta\mathcal{I})^{-1}(\mathcal{A})]_{ijkl} = \begin{cases} (\lambda + 4\beta)^{-1} A_{ijkl} & \text{if } ijkl \text{ is non-empty} \\ (4\beta)^{-1} A_{ijkl} & \text{if } ijkl \text{ is empty} \end{cases} \tag{22}$$

Therefore, the minimum of $\mathcal{D}$ is

$$\widetilde{\mathcal{D}}\big|_{ijkl} = \begin{cases} (\lambda + 4\beta)^{-1} \left[\sum_{i=1}^{4} \mathcal{W}_i + \sum_{i=1}^{4} \beta \mathcal{Y}_i + \lambda \mathcal{D}^{obs} \right]_{ijkl} & \text{if } ijkl \text{ is n} \\ (4\beta)^{-1} \left[\sum_{i=1}^{4} \mathcal{W}_i + \sum_{i=1}^{4} \beta \mathcal{Y}_i \right]_{ijkl} & \text{if } ijkl \text{ is e} \end{cases} \tag{23}$$

where we replaced $\mathcal{T}'\boldsymbol{d}^{obs} = \mathcal{D}^{obs}$ and we accounted for $\mathcal{D}^{obs}|_{ijkl} = 0$ when the bin $ijkl$ is empty

ADMM: Tensor Completion algorithm

Finally, the algorithm that solves Equation 12 reduces to

initialize $\boldsymbol{\mathcal{D}}^0$, $\boldsymbol{\mathcal{Y}}_i^0, \boldsymbol{\mathcal{W}}_i^0,\ i = 1, 2, 3, 4$ with the null tensor

for $k = 1, k_{max}$

$\boldsymbol{\mathcal{D}}^{k+1}$ as in Equation 23

for $i = 1,2, 3, 4$

$$\boldsymbol{\mathcal{Y}}_i^{k+1} = \text{fold}\left(\text{shrink}\left(\mathbf{D}^{(i)\,k+1} - \frac{1}{\beta}\mathbf{W}_i^{(i)\,k}, \frac{1}{\beta}\right)\right)$$

$$\boldsymbol{\mathcal{W}}_i^{k+1} = \boldsymbol{\mathcal{W}}_i^k - \beta\left(\boldsymbol{\mathcal{D}}^{k+1} - \boldsymbol{\mathcal{Y}}_i^{k+1}\right)$$

end

end

output is $\boldsymbol{\mathcal{D}}^{k_{max}}$

Gandy, S., B. Recht, and I. Yamada, 2011, Tensor completion and low-n-rank tensor

Example

In order to explore the performance of the proposed algorithm, we consider a simple 3D model that contains two dipping planes with normals given by

$$n_1 = (0.02, 0.05, 0.99) \quad \text{and} \quad n_2 = (0.03, 0.02, 0.99).$$

The velocities used for this test are 1500 m/s and 2300 m/s for the top and bottom planes, respectively. The intersection of these planes with the vertical axis occurs at 250 m and 1000 m. The travel-times are calculated via ray tracing in the midpoint-offset domain. The volume corresponds to a spatial tensor of size $12 \times 16 \times 12 \times 16$ (midpoints x, y-offset x, y), 512 time samples and a time sampling rate of 2 ms. Additionally, we randomly remove 50% of the traces and add random noise to produce a volume with $SNR = 1$

Example

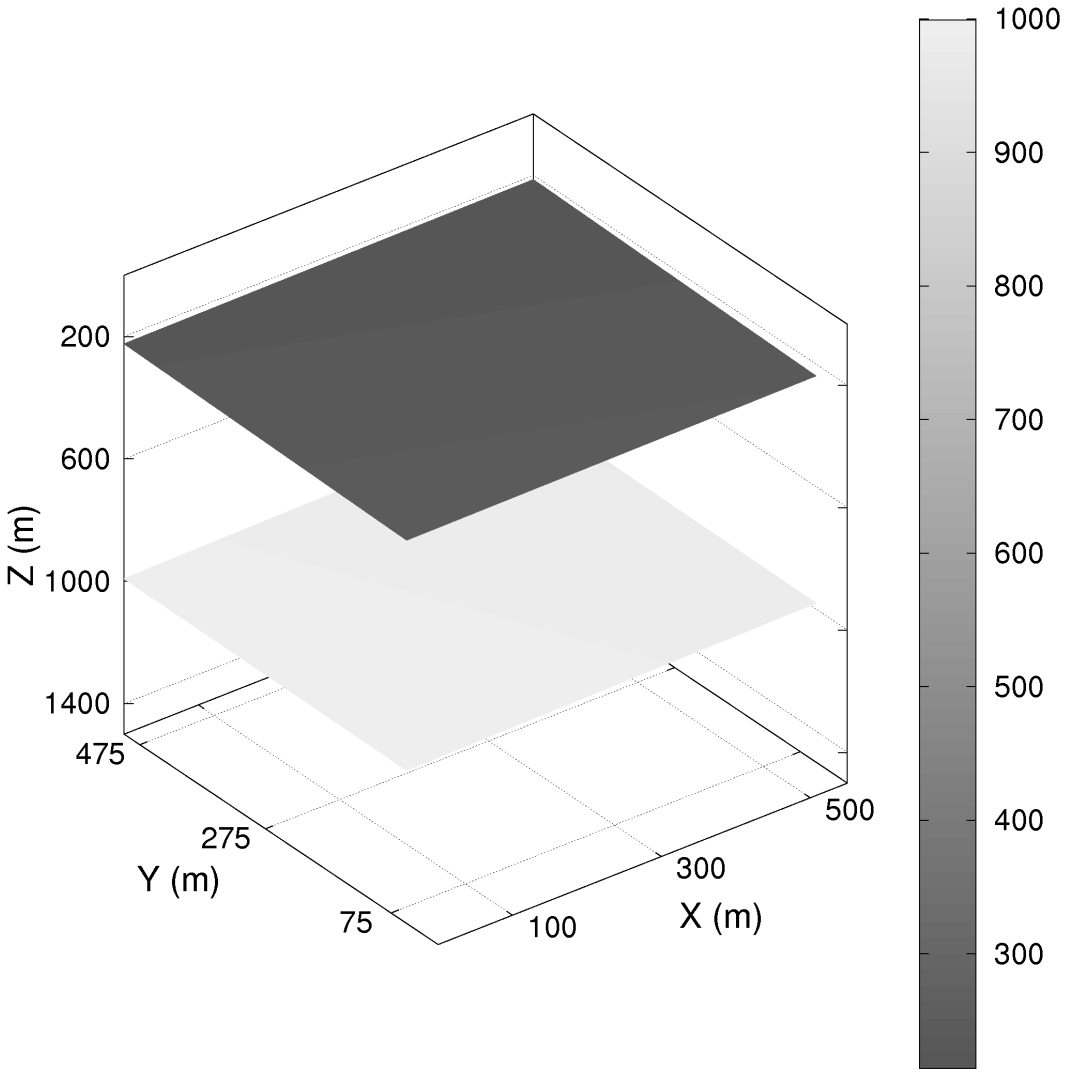

Figure: *

Example

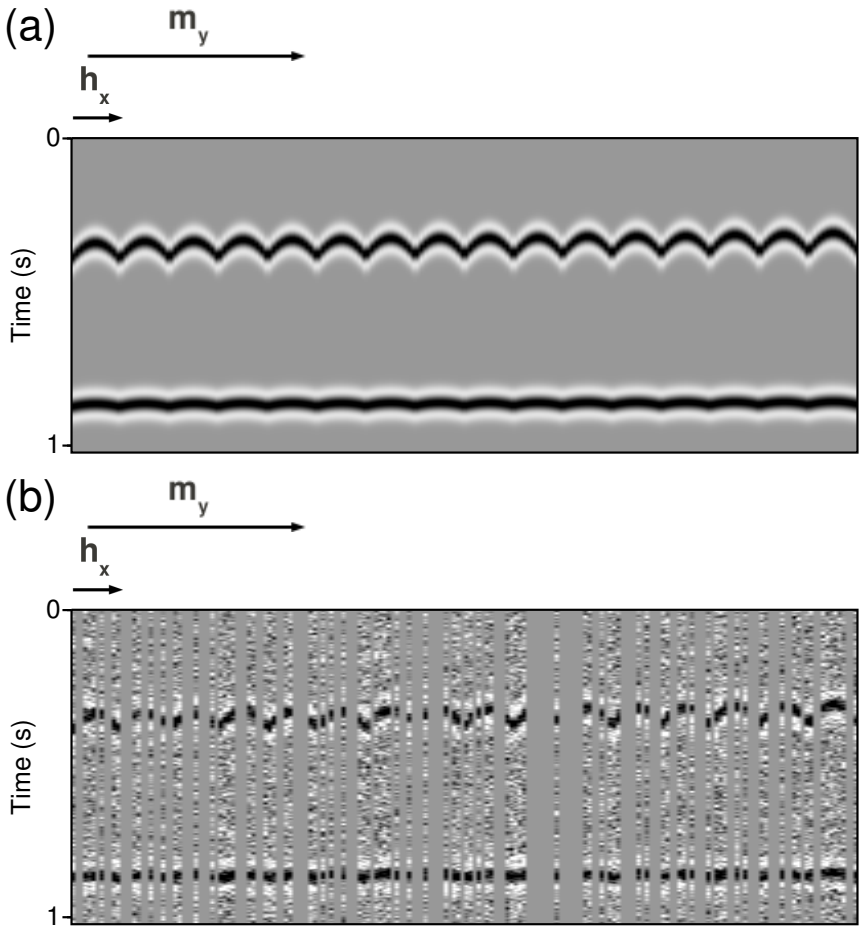

Figure: *

Example

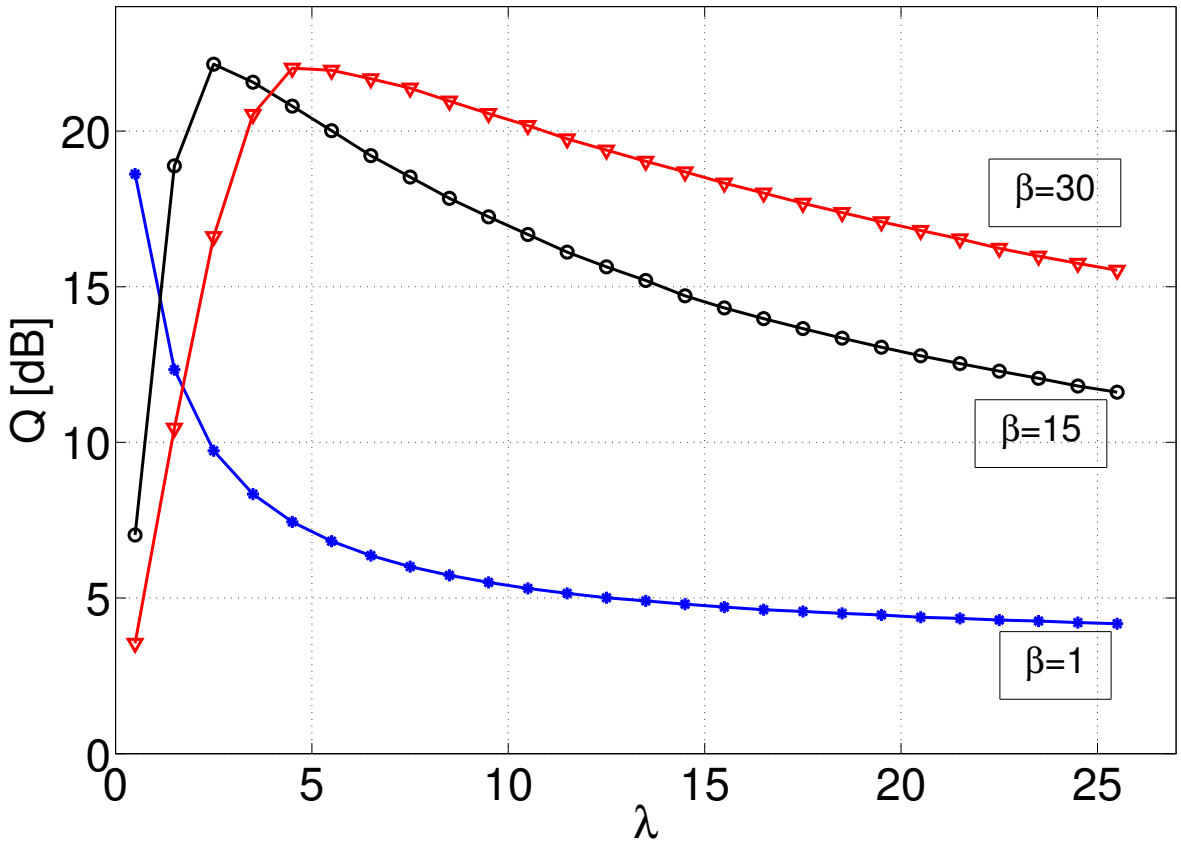

Figure: *

Quality of the reconstruction Q versus λ for $\beta = 1, 15$ and 30. A higher value of Q indicates a higher reconstruction quality. For a fixed value of β, the quality decreases as λ increases.

Example

$$n_1 = (0.26, 0.17, 0.95) \quad \text{and} \quad n_2 = (0.12, 0.16, 0.98). \quad (24)$$

The intersection of the planes with the vertical axis occurs at 350 m and 1000 m and the velocities coincide with those in the previous model. We remove 40% of the traces randomly and add randomly distributed Gaussian noise with a $SNR = 1$. The quality of the reconstruction for this case is $Q = 20$ dB and the running time is 4 h 28 min (MATLAB).

Example

Common midpoint gathers with 40% randomly decimated traces and $SNR = 1$. (a) Portion of the 5D desired volume. (b) Decimated and noisy data. This is the input to the algorithm. (c) Reconstructed data.

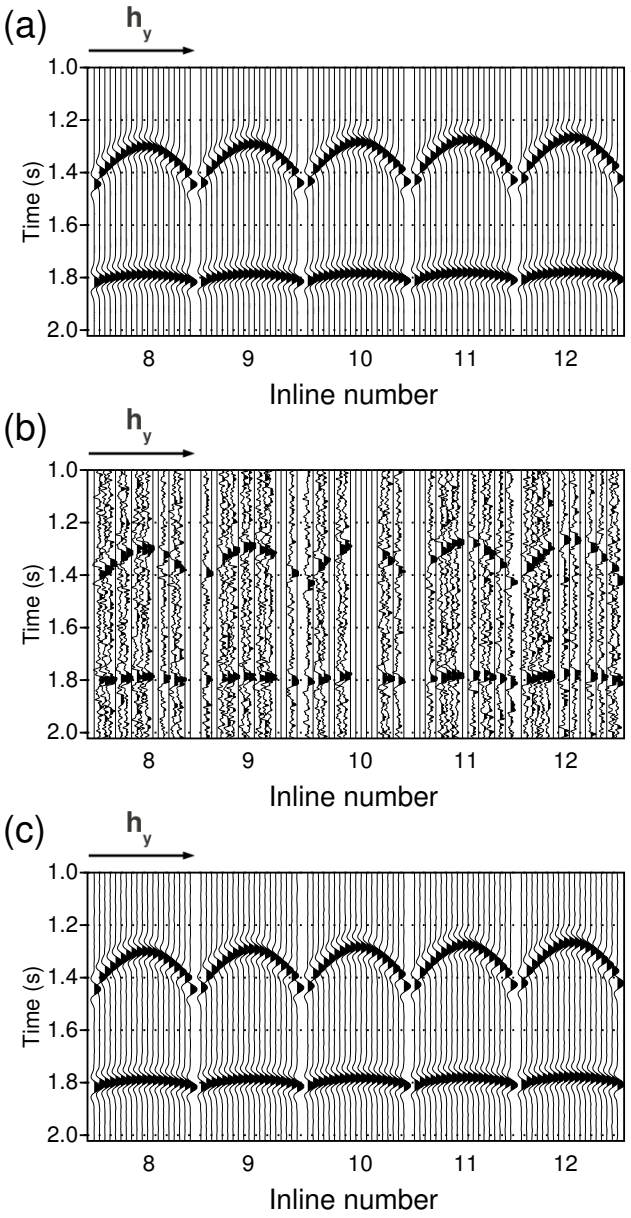

Example

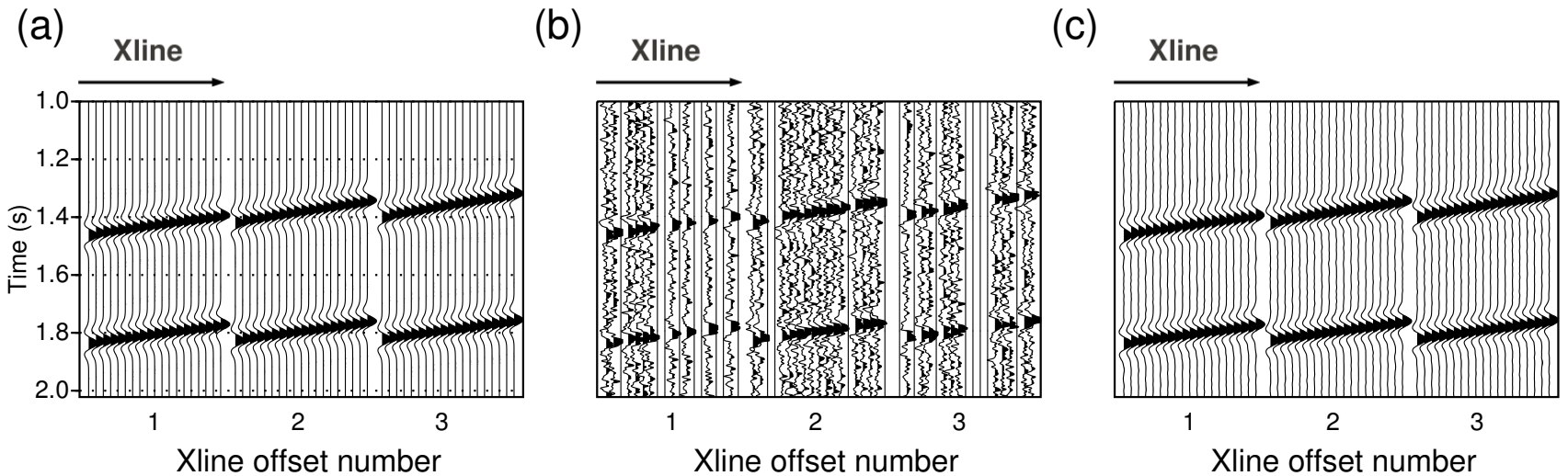

Figure: *

Common offset gathers with 40% randomly decimated traces and $SNR = 1$. (a) Portion of the 5D desired volume. (b) Decimated and noisy data. This is the input to the algorithm. (c) Reconstructed data.

Example

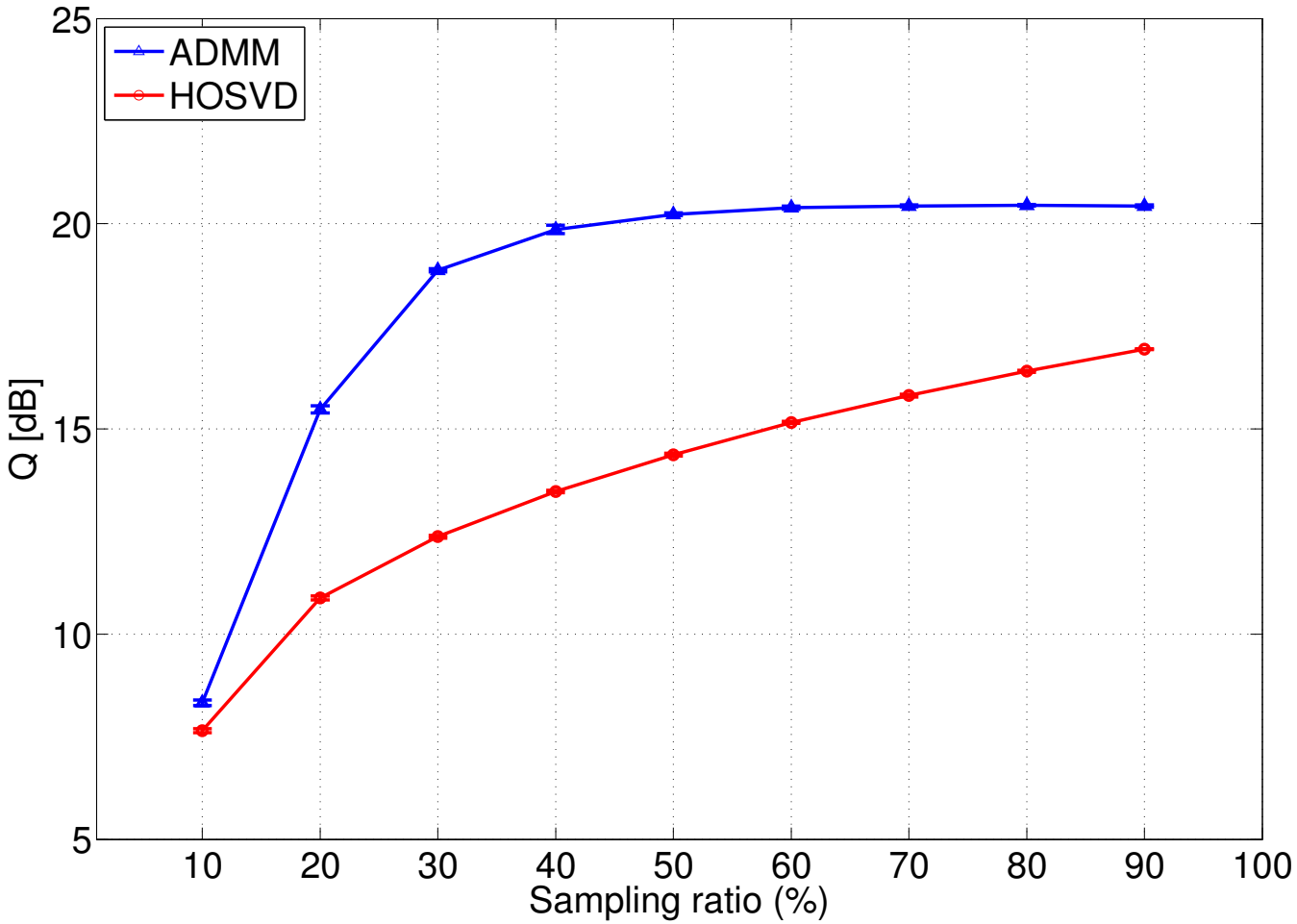

Figure: *

Quality of the reconstruction versus sampling ratio for a synthetic volume. The quality of the reconstruction increases as the sampling ratio increases for both the proposed

Field example. Data set from the WCSB

Our real data example is from an orthogonal survey acquired over a heavy oil field in Alberta, Canada. It is common practice in the reconstruction of seismic data to use overlapping windows in both space and time. We reconstruct a crossline swath from this survey by dividing it into 21 overlapping blocks of inline/crossline (13 inlines overlap length).

For each block, the dimensions of the grid are:

- Inline (CMPx): $n_1 = 26$, increment=5 m (inline overlap of 13 CMPs)
- Crossline (CMPy): $n_2 = 26$, increment=5 m
- Offset: $n_3 = 5$, increment=100 m, [min,max]=$[50, 450]$ m
- Azimuth: $n_4 = 8$, increment=45°, [min,max]=$[22.5°, 337.5°]$

Size of tensor: $26 \times 26 \times 5 \times 8$

WCSB survey

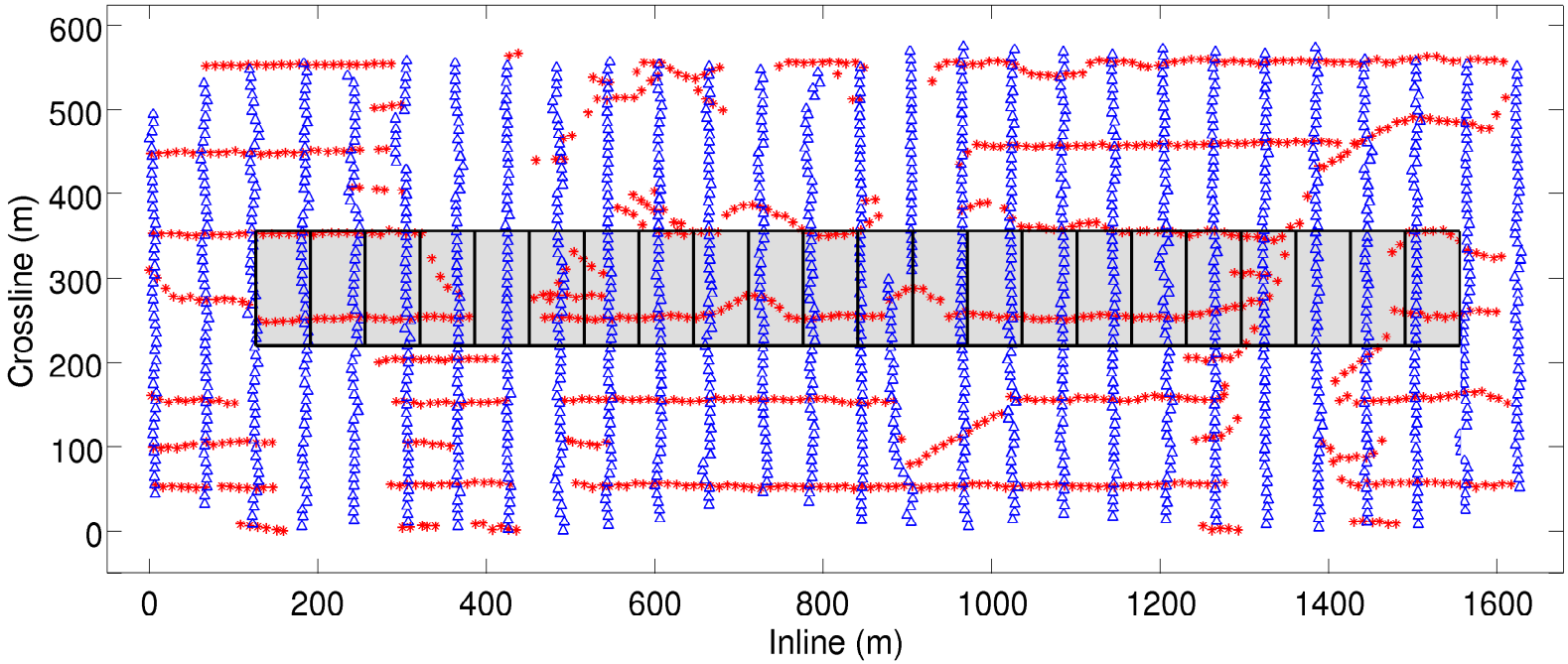

Figure: *

Survey geometry for the real data example in true aspect ratio. Stars indicate sources and triangles indicate receivers. The grey area shows the midpoints that were reconstructed with the proposed algorithm. We use 21 blocks of size 26×26 midpoints with an overlap of 13 inline cmp positions. Each block is represented by two adjacent rectangles.

WCSB survey

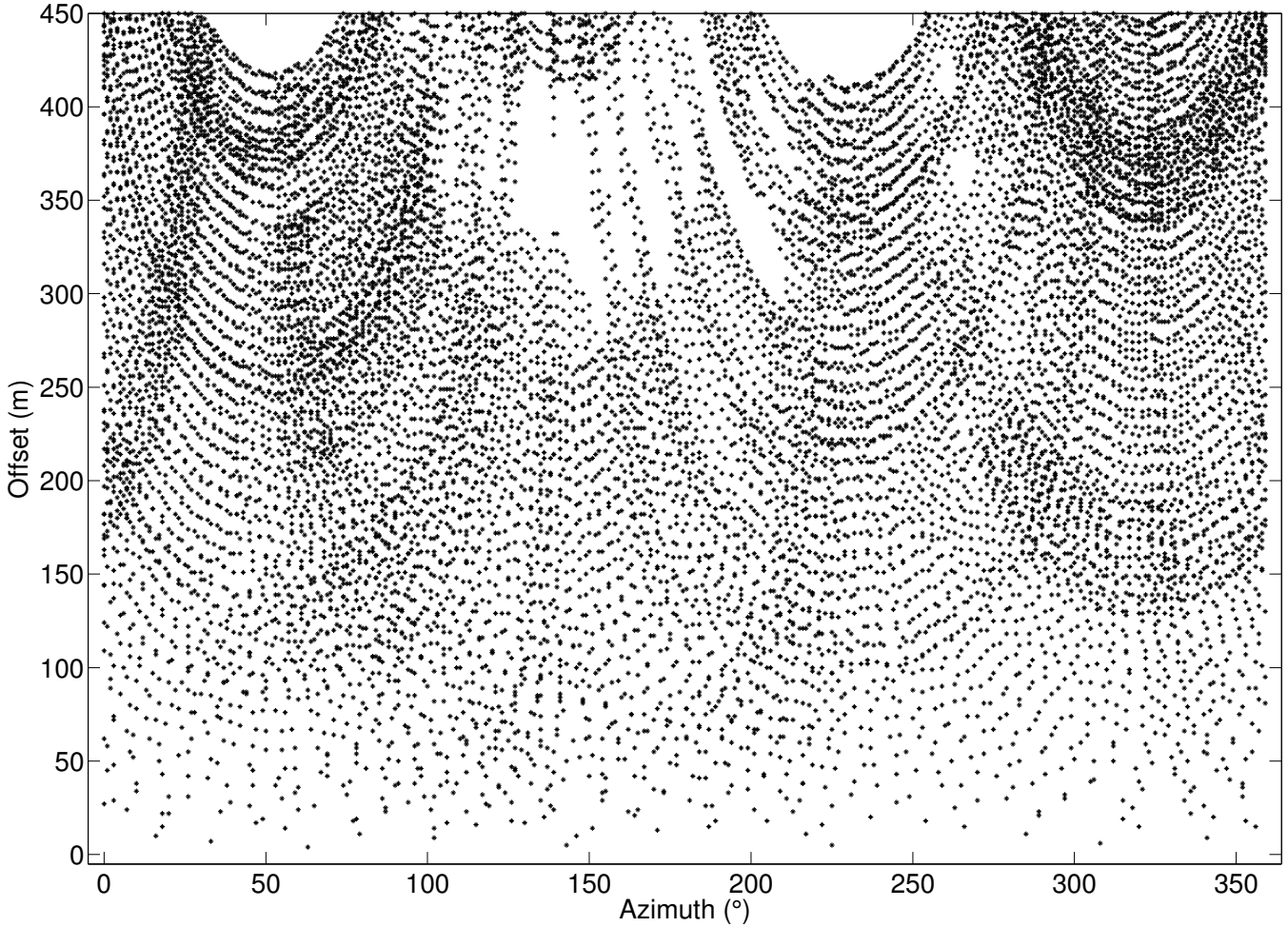

Figure: *

Offset azimuth distribution for one block of data used in the reconstruction.

WCSB survey

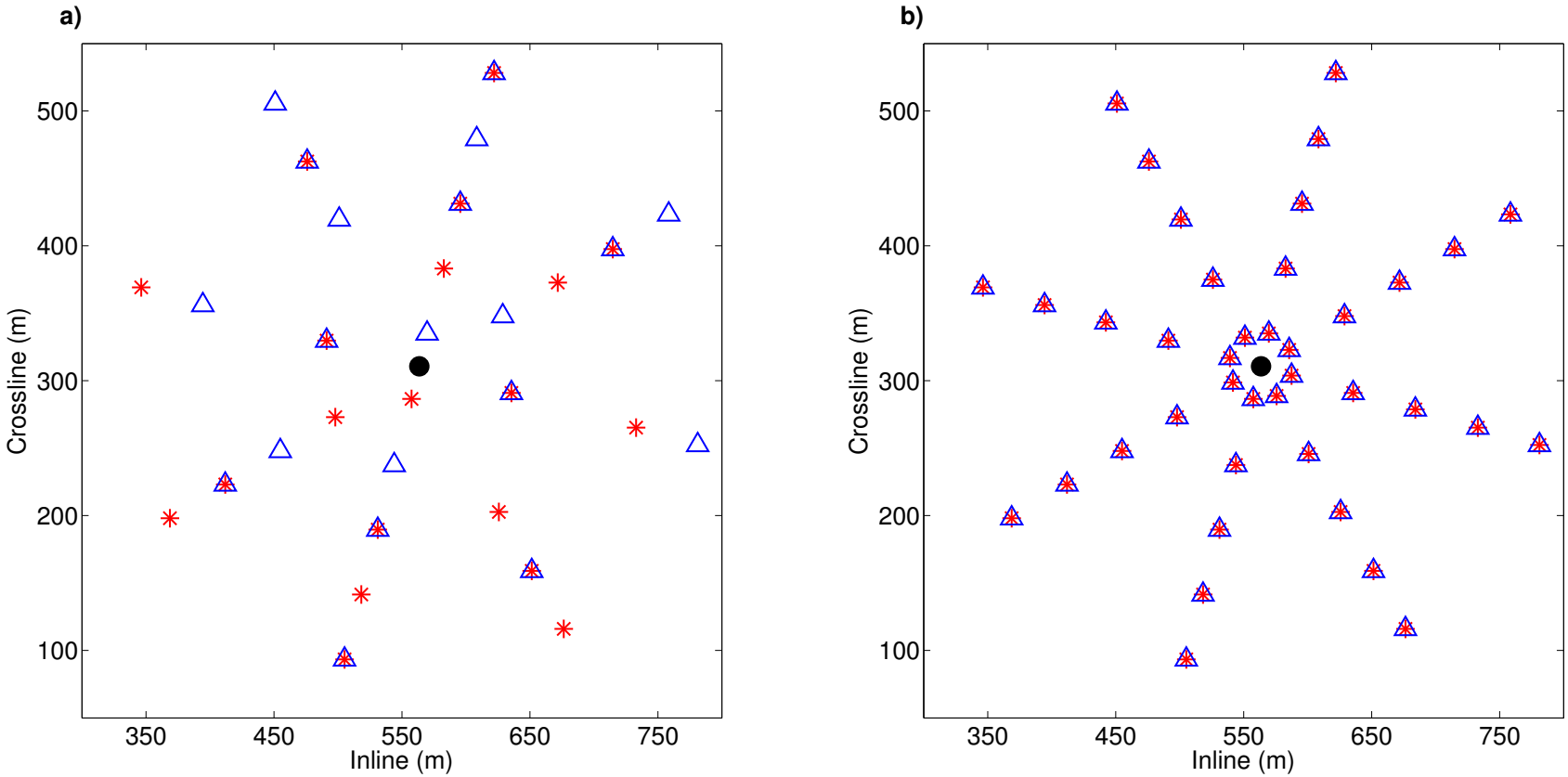

Figure: *

Source receiver geometry for the bin with its center at $(564, 311)$m. The black dot marks the position of the midpoint, triangles indicate receivers and stars indicate sources. a) Position of the available source-receiver pairs before reconstruction. b)

WCSB survey

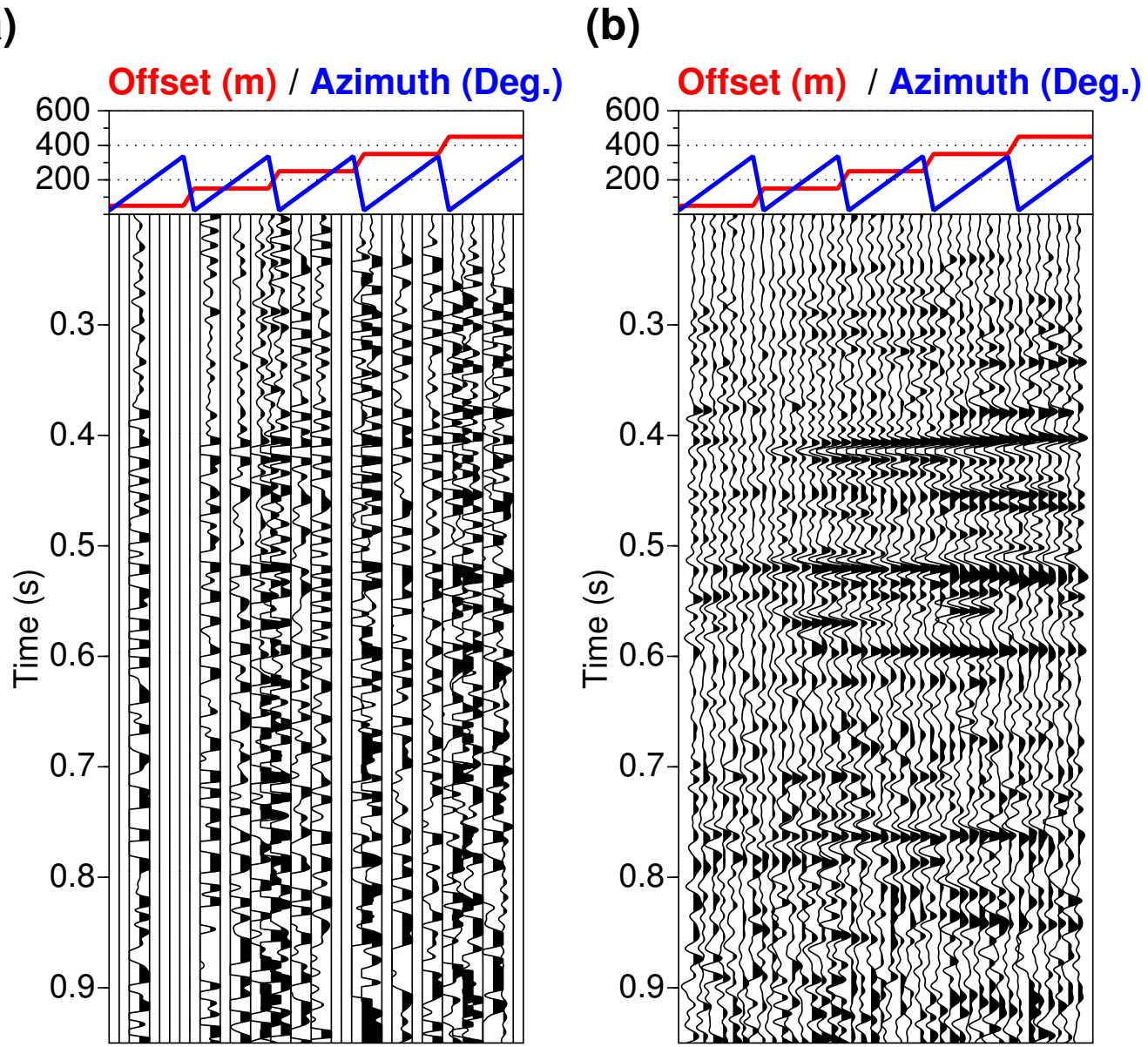

Figure: *

WCSB survey: Near offsets

Near offset gathers (50 m) for a constant crossline. Panels (a) and (b) have a constant azimuth of 22.5° while (c) and (d) have a constant azimuth of 112.5°. (a)-(c) Before reconstruction. (b)-(d) After reconstruction.

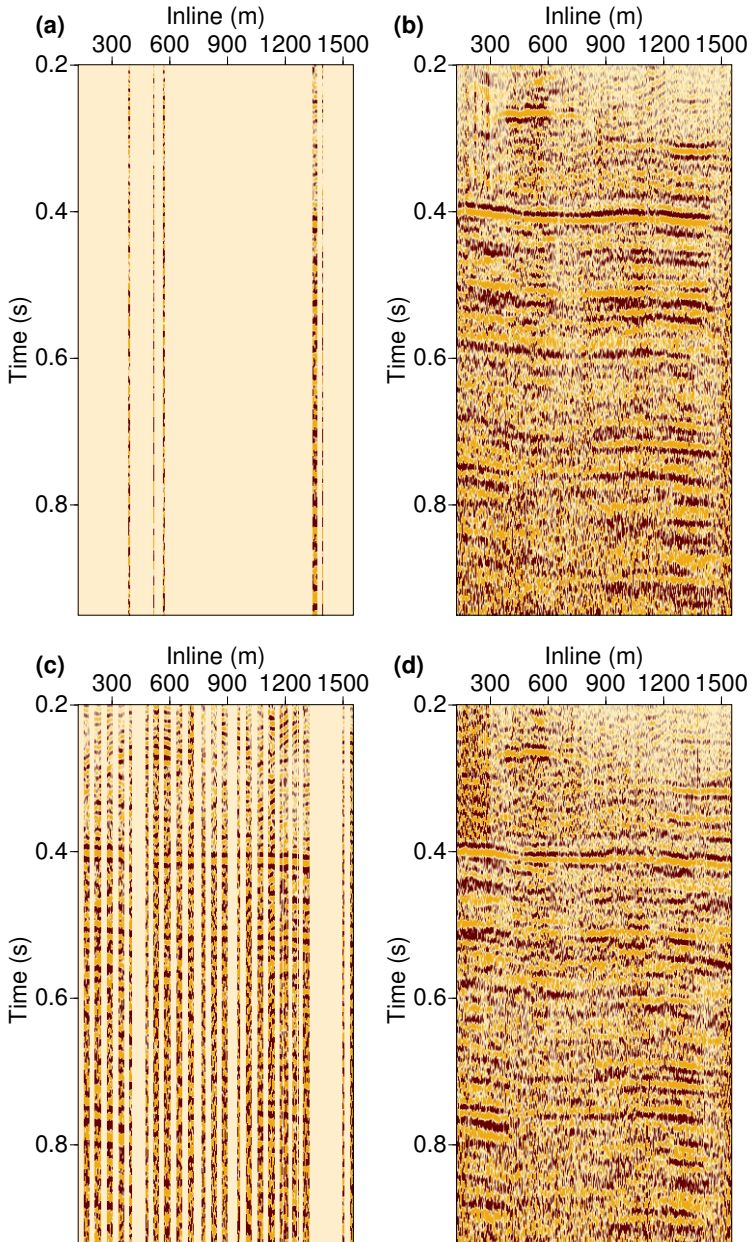

WCSB survey: Mid range offsets

Mid-offset gathers (250 m) for a constant crossline. Panels (a) and (b) have a constant azimuth of 22.5° while (c) and (d) have a constant azimuth of 112.5°. (a)-(c) Before reconstruction. (b)-(d) After reconstruction.

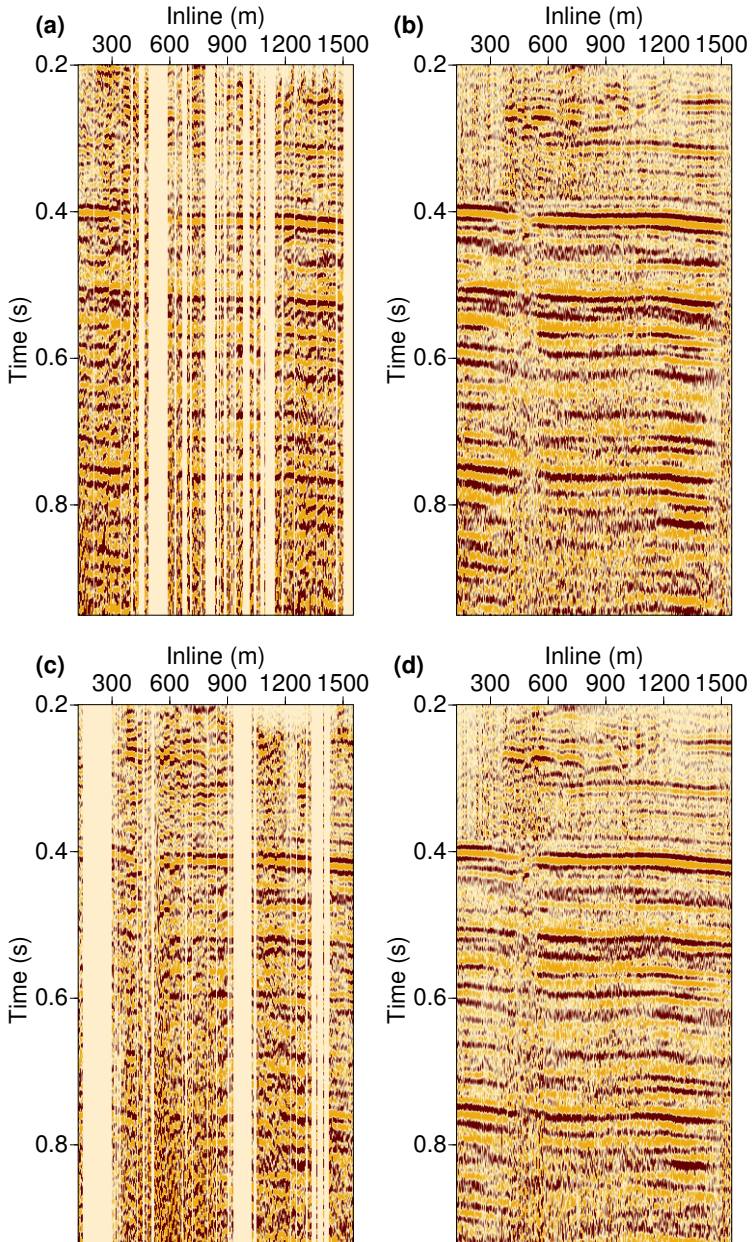

WCSB survey: Far offsets

Far offset gathers (450 m) for a constant crossline. Panels (a) and (b) have a constant azimuth of 22.5° while (c) and (d) have a constant azimuth of 112.5°. (a)-(c) Before reconstruction. (b)-(d) After reconstruction.

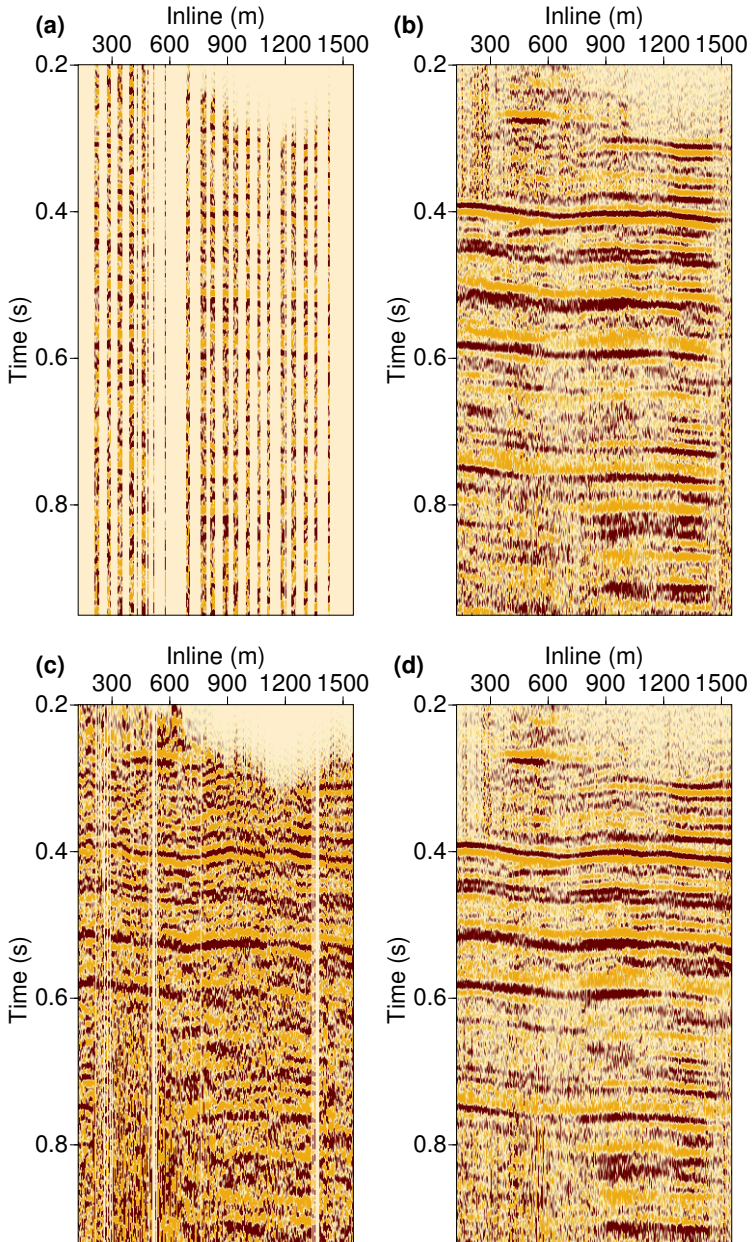

WCSB survey: Inline and crossline section stacks

Stack of all 21 blocks for a constant crossline: (a) Without reconstruction. (b) With reconstruction.

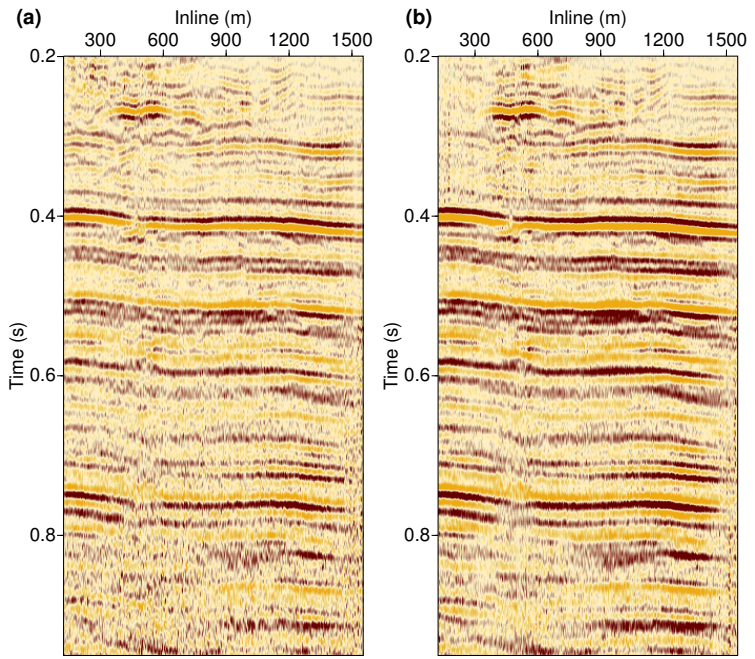

WCSB survey

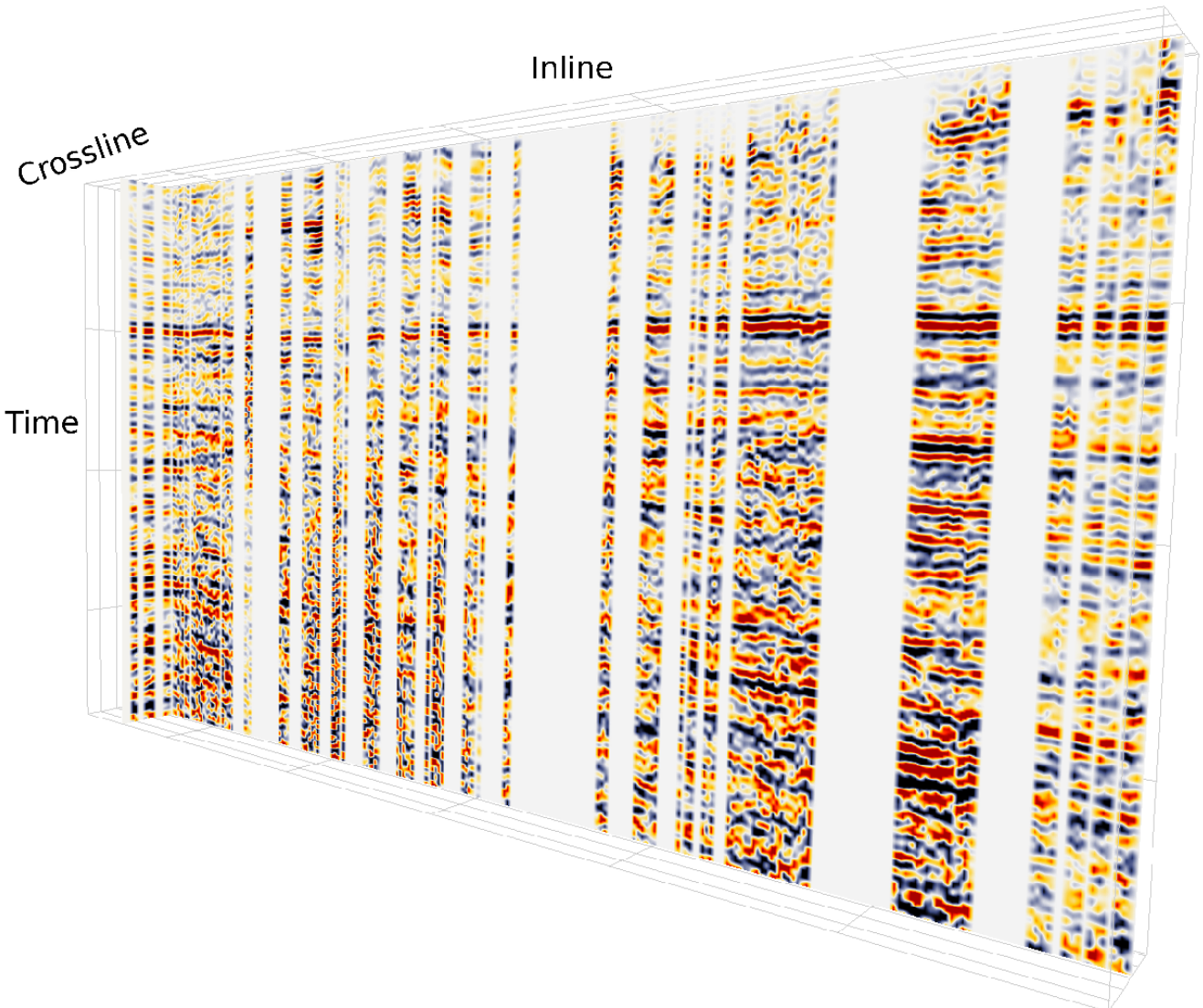

Observed volume for a constant offset (3rd offset bin) and azimuth (4th azimuth bin)

WCSB survey

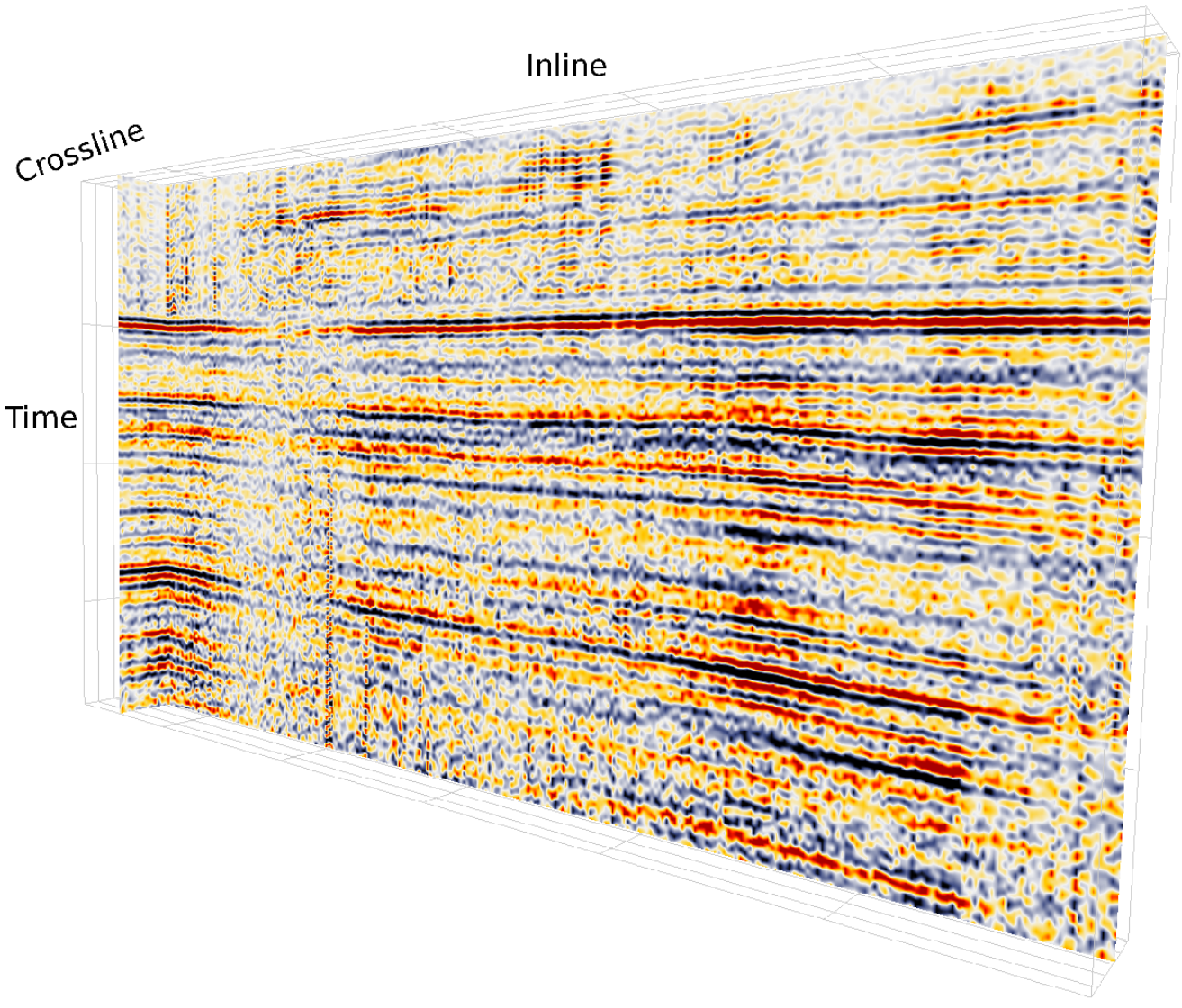

Reconstructed volume for a constant offset (3rd offset bin) and azimuth (4th azimuth

WCSB survey

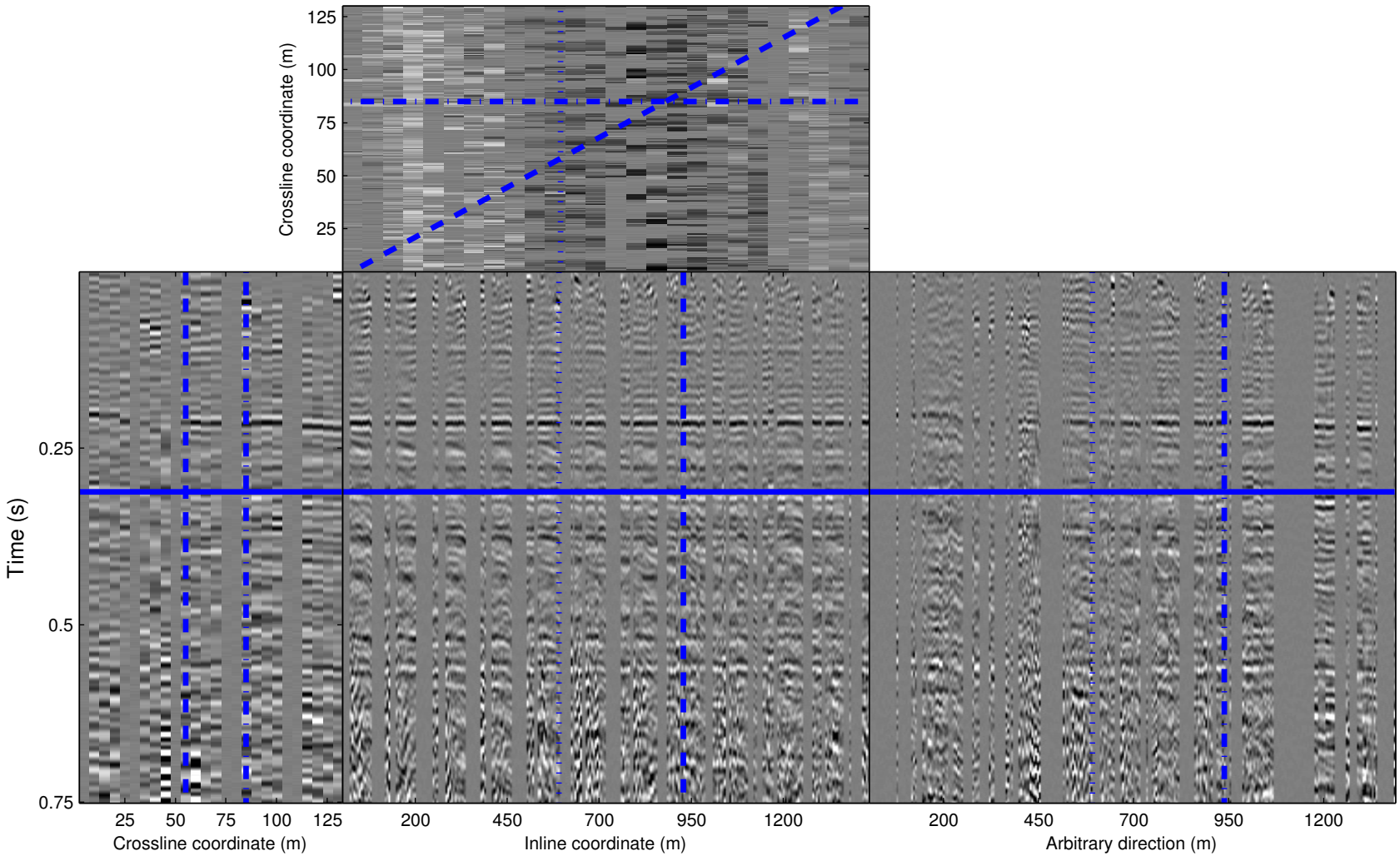
Crossline coordinate (m)
125
100
75
50
25
Time (s)
0.25
0.5
0.75
25
50
75
100
125
200
450
700
950
1200
200
450
700
950
1200
Crossline coordinate (m)
Inline coordinate (m)
Arbitrary direction (m)

WCSB survey

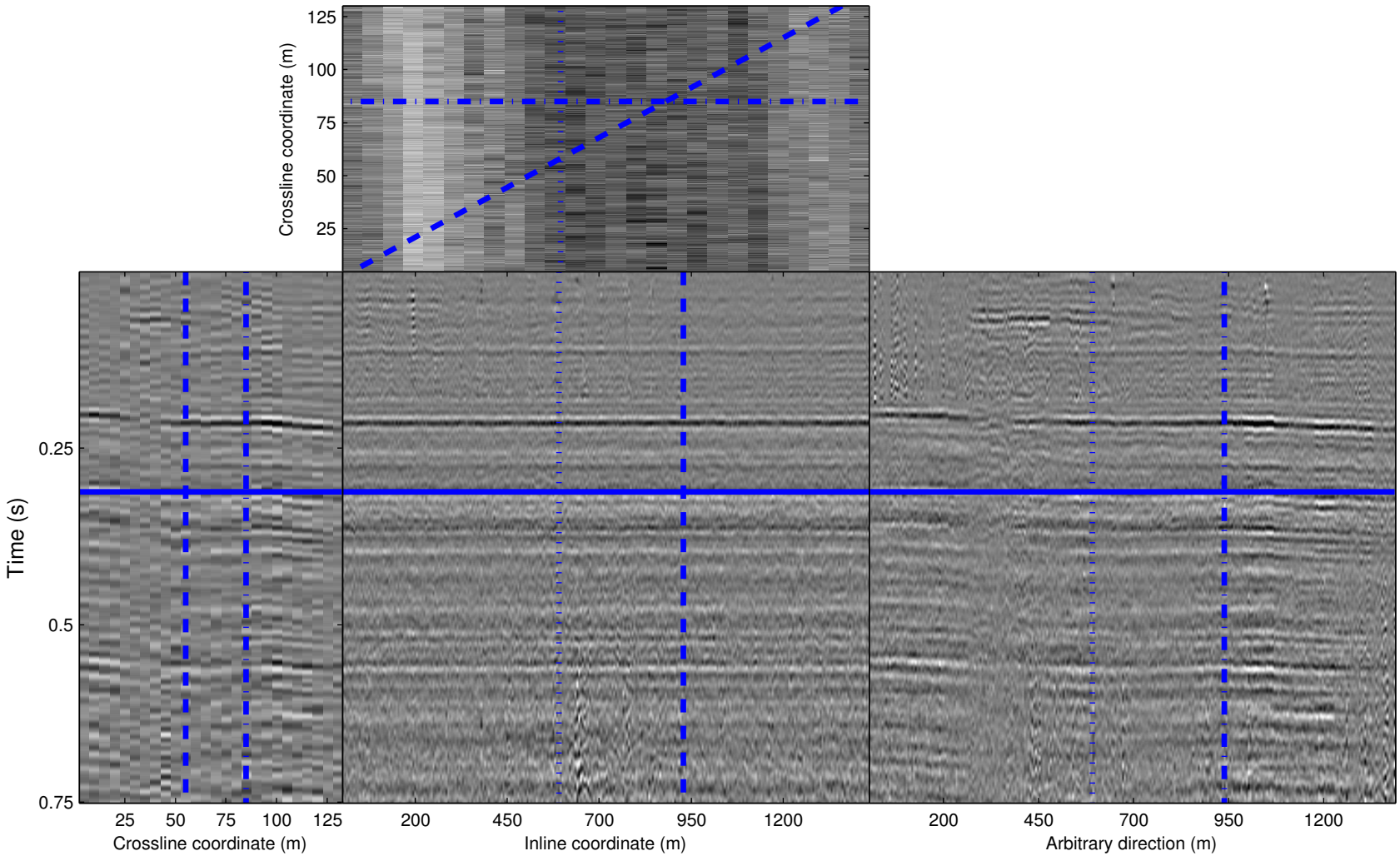
Crossline coordinate (m)
125
100
75
50
25
Time (s)
0.25
0.5
0.75
25
50
75
100
125
Crossline coordinate (m)
200
450
700
950
1200
Inline coordinate (m)
200
450
700
950
1200
Arbitrary direction (m)

Conclusions

- Rank-reduction (Hankel / Tensor) reconstruction techniques are an alternative to Fourier-based reconstruction methods
- Unlike Fourier-based reconstruction, the field does not have many players and uses interesting math that has received little attention in geophysics (Multilinear Algebra, Tensor Completion, Nuclear norm minimization, ADMM, etc..)
- Advantages: Excellent denoising capability, simultaneous data denoising and reconstruction, can cope with curvature
- Disadvantages: Computational cost
- Current direction: Solvers that do not use the SVD
- Current direction: Robust Tensor completion